Space Shuttle Orbiter Wing-Leading-Edge Panel Thermo-Mechanical Analysis for Entry Conditions

Norman F. Knight, Jr.[1]
General Dynamics Information Technology, Chantilly, Virginia

Kyongchan Song[2]
ATK Space Division, Hampton, Virginia

Ivatury S. Raju[3]
NASA Langley Research Center, Hampton, Virginia

Linear elastic, thermo-mechanical stress analyses of the Space Shuttle Orbiter wing-leading-edge panels is presented for entry heating conditions. The wing-leading-edge panels are made from reinforced carbon-carbon and serve as a part of the overall thermal protection system. Three-dimensional finite element models are described for three configurations: integrated configuration, an independent single-panel configuration, and a local lower-apex joggle segment. Entry temperature conditions are imposed and the through-the-thickness response is examined. From the integrated model, it was concluded that individual panels can be analyzed independently since minimal interaction between adjacent components occurred. From the independent single-panel model, it was concluded that increased through-the-thickness stress levels developed all along the chord of a panel's slip-side joggle region, and hence isolated local joggle sections will exhibit the same trend. From the local joggle models, it was concluded that two-dimensional plane-strain models can be used to study the influence of subsurface defects along the slip-side joggle region of these panels.

I.   Introduction

The overview of the Space Shuttle Orbiter shown in Fig. 1 depicts the structural layout of the wing internal structure as well as representative wing-leading-edge (WLE) panels and their associated T-seal. Stiffness of the wing structural subsystem (wing spars and ribs) varies along the wing span. The leading edge of each wing has twenty-two reinforced carbon-carbon (RCC) panel/T-seal sets. These WLE panel assemblies are designed to provide aerodynamic performance and to provide thermal protection on entry. The WLE structure is exposed to mechanical and acoustic loading and possible debris impact during every mission. On entry, the WLE is subjected to aerothermodynamic loading during the heat-pulse phase of entry and then mechanical loading by aerodynamic pressure during final phase of entry prior to landing. WLE Panels 8, 9, and 10 typically experience the highest entry temperatures.
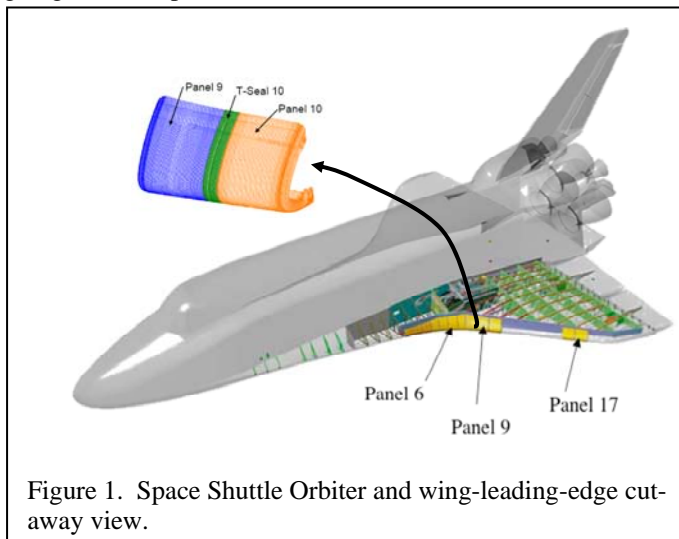

Figure 1. Space Shuttle Orbiter and wing-leading-edge cut-away view.

---

[1] Principal Subject Matter Expert. Fellow AIAA. Fellow ASME.
[2] Structural Analyst. Member AIAA.
[3] NASA Technical Fellow for Structures, NASA Engineering and Safety Center. Fellow AIAA. Member ASME.

1
American Institute of Aeronautics and Astronautics

Global three-dimensional thermo-mechanical stress analyses [1, 2] are performed for Panel 9, T-seal 10, and Panel 10 (see Fig. 2) to assess the three-dimensional nature of the response using entry conditions for selected times after entry interface. These analyses are performed using the ABAQUS/Standard finite element code [3] and provide the overall structural response. This paper examines the global three-dimensional thermo-mechanical elastic stress analysis models of the WLE panels to investigate the thermo-mechanical response to entry conditions and to determine appropriate simplifying assumptions for subsequent fracture mechanics analysis [4, 5].
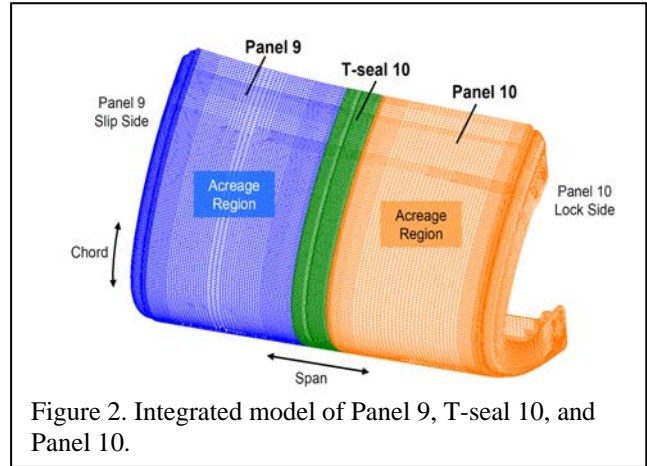

Figure 2. Integrated model of Panel 9, T-seal 10, and Panel 10.

In the present paper, the three different configuration models shown in Fig. 3 are summarized. These configurations include the integrated model, the single-panel model, and a local region model. The integrated model involved Panels 9 and 10 as well as T-seal 10. The single-panel model involves only Panel 10. The local region model involves an isolated local 4-inch × 4-inch segment from the lower-apex slip-side joggle region of Panel 10. The objective of this paper is to assess the modeling and analysis requirements for accurate prediction of the through-the-thickness structural response along the slip-side joggle region of the Space Shuttle Orbiter WLE panels for entry conditions.
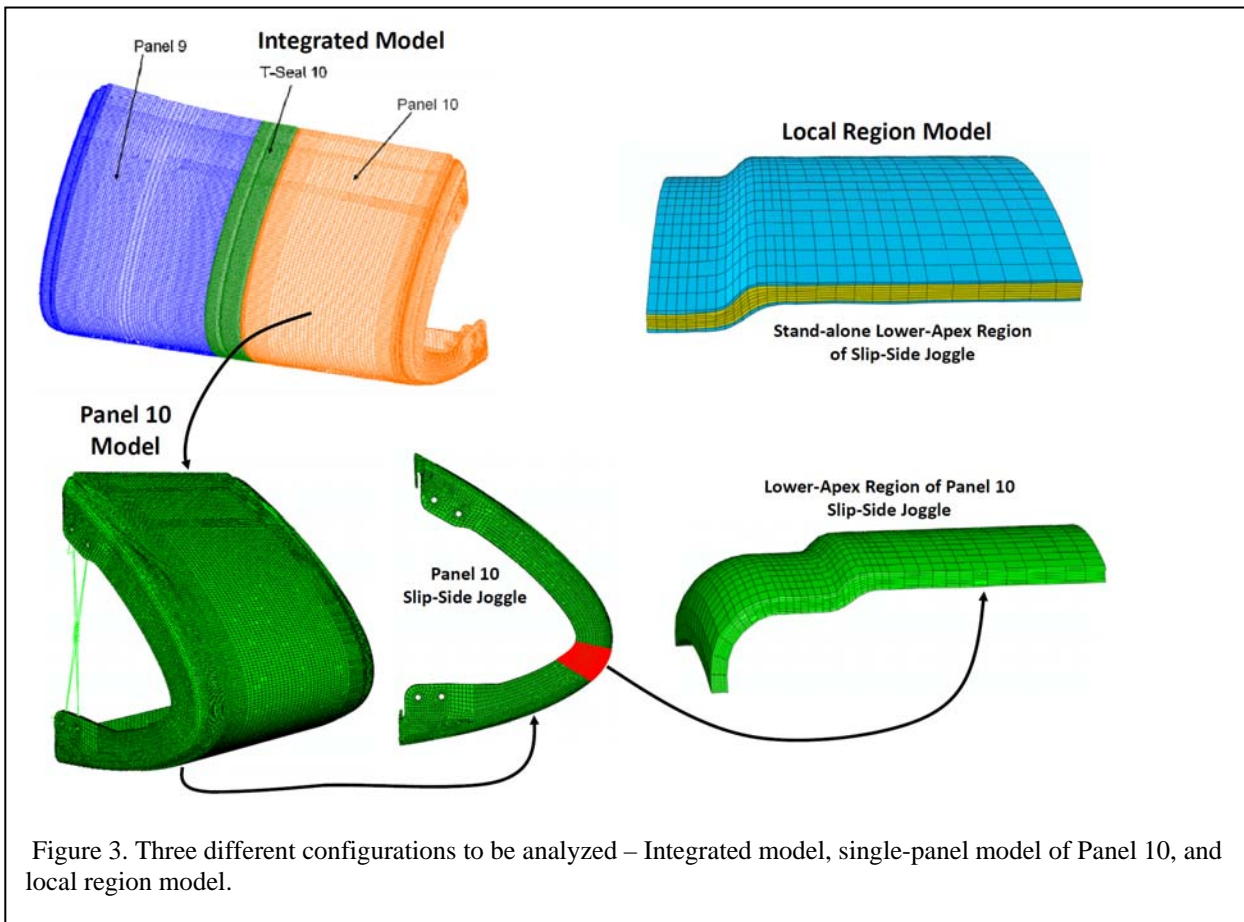

Figure 3. Three different configurations to be analyzed – Integrated model, single-panel model of Panel 10, and local region model.

American Institute of Aeronautics and Astronautics

II.   Analysis

Global three-dimensional (3D) models of a WLE panel that had higher fidelity along the joggle regions than elsewhere in the panel were developed using a building-block approach [1]. The building-block approach begins with basic elements and builds in complexity in a systematic, progressive manner. Such an approach permits each step in the process to be verified and its influence on the overall response determined. This section described the finite element modeling approach, the boundary conditions, the material modeling, and the thermal loading conditions.

A. Finite Element Modeling

The finite element modeling of WLE Panels 9 and 10 is based on different strategies as illustrated in Fig. 4 using Panel 10. The first modeling strategy is based on using four three-dimensional 8-node hexahedral solid elements through the thickness everywhere in the panel (Model P10B4). The second modeling strategy attempts to increase the acreage response fidelity by using shell elements, while retaining four solid elements on both the slip-side and lock-side joggle regions (Model P10C4). The third modeling strategy further increases the modeling fidelity over the second strategy by increasing the number of elements in the through-the-thickness direction to eight in the slip-side joggle region only (Model P10C8). The higher fidelity along the joggle region included discrete layer modeling of the coating and substrate material through the RCC thickness.
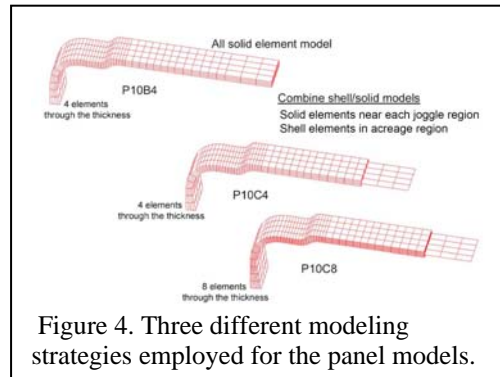

Figure 4. Three different modeling strategies employed for the panel models.

The finite element modeling of T-seal 10 is based on 8-node solid hexahedral elements with four elements through the thickness, see Fig. 5. Because the T-seal and the panel joggle regions are represented using three-dimensional solid elements, surface contact and surface interactions are readily and explicitly defined using the bounding surfaces.
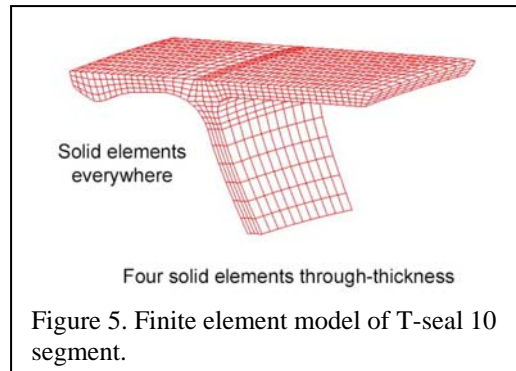
Each RCC component model with four solid elements through the thickness use homogeneous or laminated RCC material properties. However, along the slip-side joggle region with either elements through the thickness, discrete layers of coating material and substrate material are defined. Such a modeling approach permits the simulation of the thermal mismatch between coating and substrate for thermo-mechanical stress analyses.

Figure 5. Finite element model of T-seal 10 segment.

B. Boundary Conditions

Each RCC panel assembly attaches to the WLE front spar through a series of four attachments as indicated in the schematic shown in Fig. 6. The panel and T-seal from the outboard side or lock-side of the wing comprise a panel/T-seal set. The attachment points are referred to as the upper and lower field-break attachment points on the inboard or slip side and the outboard or lock side of the panel. The outboard side of the panel also has a shear fitting attachment (shear lug region) on the panel's upper and lower rear spars.

Attachment hardware for a WLE panel assembly consists of the clevis fittings that attach the WLE panels to the WLE front spar attachment fittings, the moment ties (or spanner beams) that connect to the lugs on the panel upper and lower edges on the inboard and outboard sides, and the clevis fittings that attach the T-seal to the lock side of the panel.   The engineering analysis models for the WLE panel attachment hardware consist of bar elements, linear springs, and multi-point constraints. These engineering analysis models are incorporated with the global three-dimensional finite element models [2].

American Institute of Aeronautics and Astronautics

The WLE front spar and spar attachment fittings are not modeled directly in either the certified global shell models or the global three-dimensional models, but rather their stiffness is represented by the direct matrix input at grids (DMIG) of stiffness coefficients (i.e., DMIG terms in MSC.Nastran jargon) at each field-break point (FBP) and shear fitting as indicated in Fig. 6. These stiffness coefficients for the different FBPs represent the stiffness of the WLE structural subsystem at that location along the WLE structure.
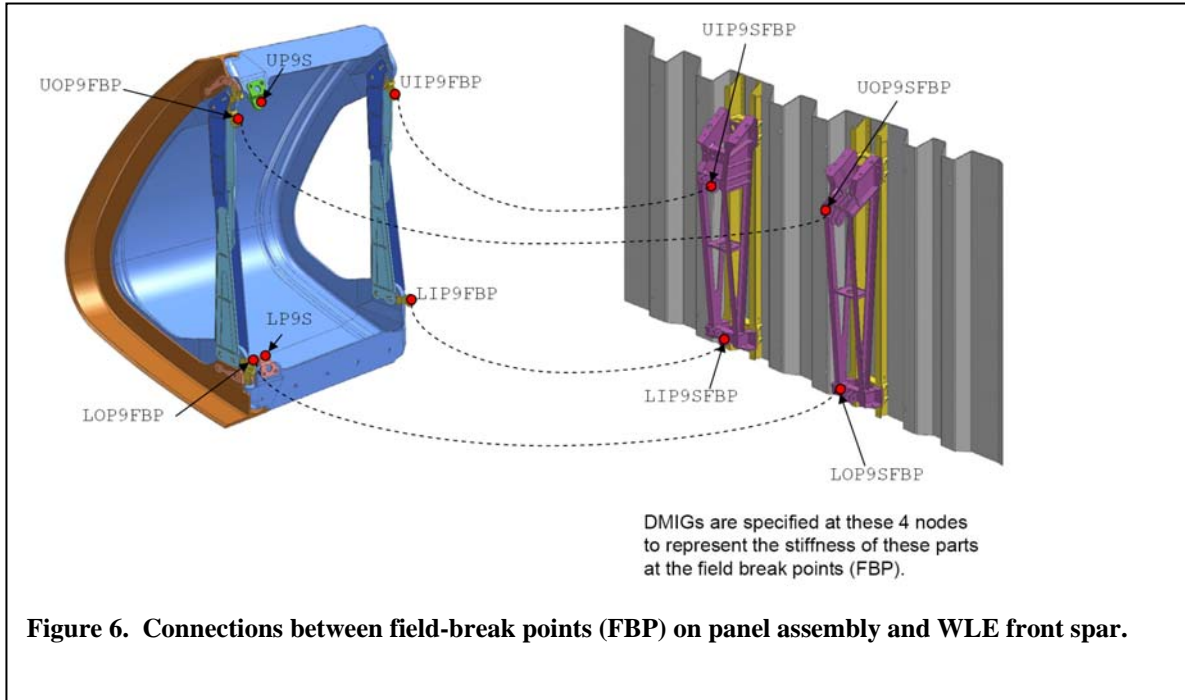

Figure 6. Connections between field-break points (FBP) on panel assembly and WLE front spar.

C. Material Modeling

RCC material serves as part of the Space Shuttle thermal protection system with a maximum operating temperature of 3000°F. The structural analyses incorporate three material modeling approaches of coated RCC components [1]. One approach to coated RCC material modeling is to smear (or average) the laminate properties over the entire thickness. In this approach, the material is still treated as transversely isotropic with bi-modulus, temperature-dependent properties. However, since the material is homogeneous through the thickness, no mismatch in properties occurs. The local coated RCC thickness is determined based on the local difference between the outer and inner mold lines, and the coated RCC material properties corresponding to that local thickness are assigned.

A second approach to coated RCC modeling is to model the constituent layers discretely (i.e., like a sandwich composite) but to treat each constituent (coating or substrate) as having uniform homogeneous properties. In this approach, the coating layers and the substrate layers are assigned separate material properties, and a mismatch in material properties occurs at the coating-substrate material interface. For the coating layers, the craze cracks in the coating are in effect 'smeared' throughout the coating layer by using a near-zero in-plane elastic moduli for tension along with the actual elastic moduli for in-plane compression and for through the thickness.

A third approach to coated RCC modeling is to model the coated RCC as discrete layers as previously mentioned but to account for the coating craze cracks explicitly by actually modeling the presence of the craze cracks. In this approach, the modeling is significantly more complex and involves defining contact surfaces and contact boundary conditions for every craze crack. As a result, 'islands' of coating material are created in the model and assigned the in-situ material properties, rather than homogenous or smeared, while the substrate layers have the same properties as in the second approach.

In each coated RCC material modeling approach, the bi-modulus, transversely isotropic behavior of the coated RCC and its constituent materials are included in the material model. In addition, the effect of the stress-free temperature [6] is accounted for in the thermal strain calculations in each approach. Because coated RCC requires a non-

traditional engineering material model, a user-defined material model for ABAQUS/Standard was developed as a UMAT subroutine [7]. This subroutine addressed temperature-dependent, linear elastic orthotropic materials that exhibit a different behavior in tension and compression (i.e., bi-modulus response) for both shell and solid finite elements. For the thermo-mechanical elastic stress analyses presented in this report, the UMAT subroutine [7] computes thermal strains accounting for a stress-free temperature.

D. Thermal Loading

The global 3D model was analyzed for entry heating cases. The entry environment for the WLE panels involves primarily thermal loading as the aerodynamic pressures are low until well after peak heating has occurred. The entry environment is defined by the entry trajectory for each mission. For this investigation, the WLE entry temperature distributions are associated with a representative end-of-mission trajectory, see Ref. 1. This trajectory is used as a common basis for analysis and testing and represents a bounding entry thermal load case. Using this trajectory, transient thermal analyses are performed and temperature distributions across the panels and T-seals are predicted as a function of time after entry interface. Specific temperature distributions from two selected times after entry interface, as well as a uniform thermal condition, are imposed on the global three-dimensional model. The temperature distribution when peak temperatures occur is shown in Fig. 7 and indicates the highest temperatures occur on the panel surfaces below the panel apex. For these simulations, the temperatures were assumed to be constant

Figure 7. Entry temperature distribution at time of peak temperature.

through the thickness of the RCC components. In the present paper, three thermal loading conditions applied to the global three-dimensional thermo-mechanical stress analysis model are described.
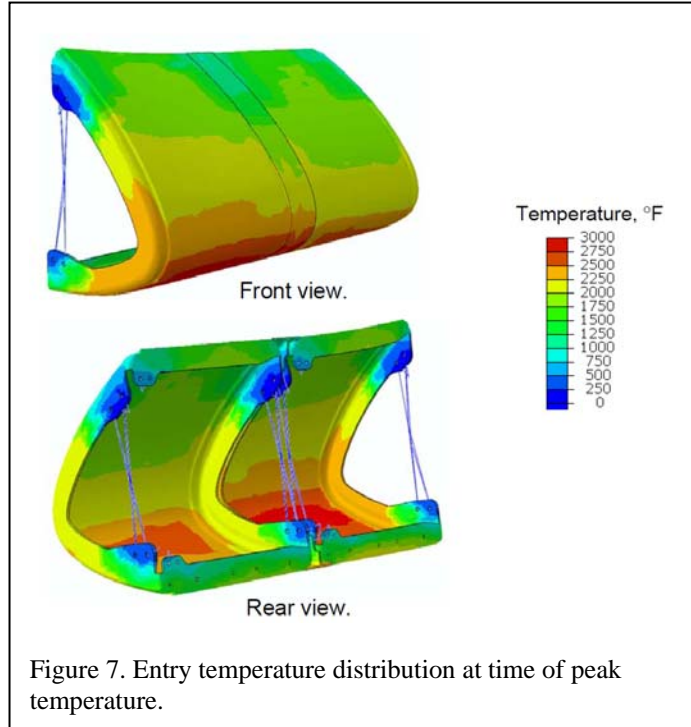
III.   Results and Discussion

In this section, selected results from the integrated global models are presented to indicate that analyzing an individual panel is sufficient for the entry heating environments because minimal contact interaction occurs between the adjacent T-seal and the panel slip-side joggle region. In addition, results from a global analysis of Panel 10 are presented and indicate that the increased values of the through-the-thickness stress component occur along the slip-side joggle all along the chord direction. Finally results are presented for a local three-dimensional model of the lower apex region of Panel 10 indicating that a two-dimensional plane-strain approach can be used for detailed subsurface defect investigations using fracture mechanics concepts.

A.   Integrated Model of Panels 9 and 10 and T-seal 10

Interaction between the WLE panel edges with the T-seal flanges (see Fig. 8) was assumed to occur for the entry thermal loading conditions – in a manner similar to their interaction when subjected to ascent or descent aerodynamic surface pressure loadings. Therefore, the thermo-mechanical stress analysis effort was directed towards the development of integrated global three-dimensional stress analysis models that included at least two WLE panels and their associated T-seal, as shown in Fig. 2. Using these global three-dimensional models, panel/T-seal interaction could be readily assessed. Details of these simulations are given in Ref. 1.
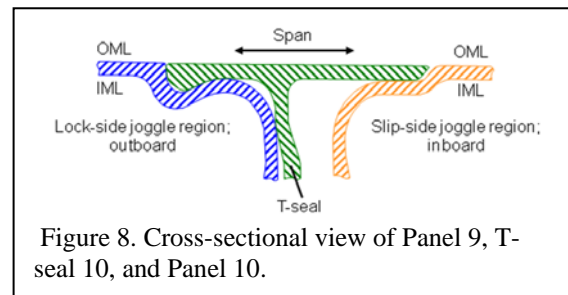

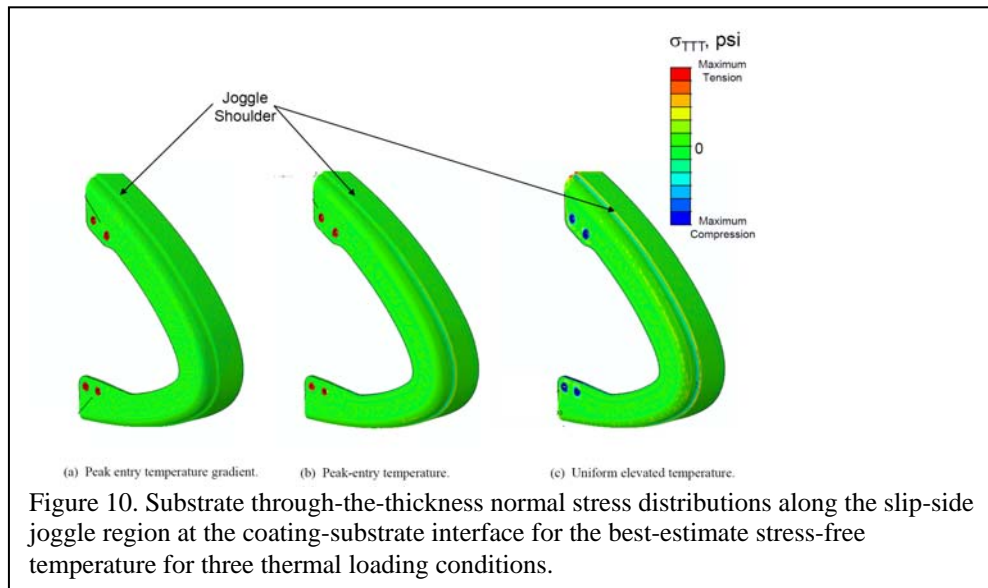Figure 8. Cross-sectional view of Panel 9, T-seal 10, and Panel 10.

The simulations using the predicted entry temperature distributions indicate that interaction between the edges of adjacent WLE panels and the intermediate T-seal are *minimal* for the thermal loading conditions analyzed. This trend also appears to be independent of the stress-free temperature assumption. Contact surface pressure distributions shown in Fig. 9 support this finding. As a result, only the isolated Panel 10 by itself and its associated attachment hardware is considered in subsequent global thermo-mechanical stress analyses of entry heating environments given in the present paper.

Figure 9. Contact modeling and contact surface pressure indications for integrated model.
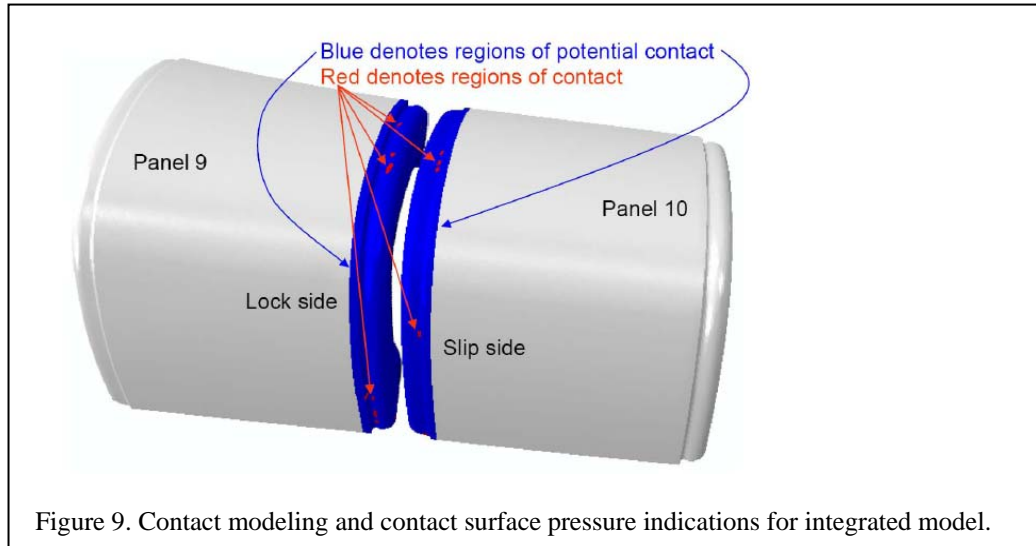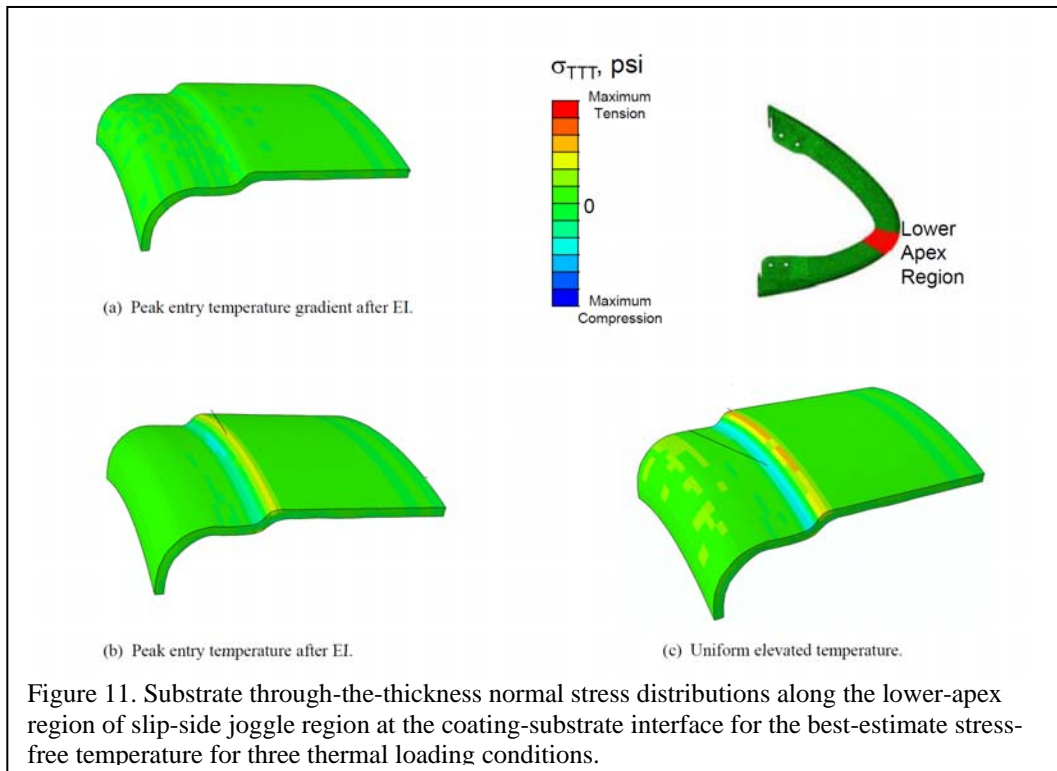
B.   Independent Single-Panel Model of Panel 10

From the integrated stress analysis results, it was concluded that the WLE panels respond independently for the entry thermal loading cases. The present assessment is focused on the inboard panel edge or slip-side joggle region of a WLE RCC panel. Along the slip-side joggle region, the global panel model has eight 8-node solid elements through the thickness, and discrete layers of homogeneous coating and substrate are represented.

Results for the overall slip-side joggle region and for lower-apex slip-side joggle (highlighted in red in the lower middle of Figure 3) are summarized in the present paper (see Refs. 1 and 8 for details). These models simulate the actual panel configuration and boundary conditions provided by the attachment hardware to the WLE front spar [2], internal loads, and local support provided by the surrounding material. Hence, these models can identify the thermo-mechanical stress and strain states that need to be simulated when using an isolated lower-apex local model.

Figure 10. Substrate through-the-thickness normal stress distributions along the slip-side joggle region at the coating-substrate interface for the best-estimate stress-free temperature for three thermal loading conditions.

American Institute of Aeronautics and Astronautics

Three thermal conditions are analyzed using the Panel 10 model and correspond to non-uniform entry temperature distributions from two time slices after entry interface (EI) and to a uniform elevated-temperature condition (i.e., all nodes in the finite element model are assigned the same temperature). Stress analysis results for the thermal conditions presented in Ref. 1 using the ABAQUS/Standard C3D8I solid element are summarized in this paper. The substrate through-the-thickness normal stress σ_{TTT} distributions shown in Fig. 10 for the overall slip-side joggle region indicate a very low stress level for all three thermal conditions. In addition, the highest σ_{TTT} stress levels are indicated at the panel lugs where the fittings are attached. Close-up views of this stress distribution on the lower-apex region are shown in Fig. 11. For the uniform temperature case, the σ_{TTT} distribution shows increased tensile values at the slip-side joggle shoulder *all* along the chord. Second, the substrate stress distribution appears to be nearly independent of the chord location with only a spanwise gradient evident, even though a uniform thermal condition is applied. Third, a band of high compressive through-the-thickness stress is evident at the bottom of the joggle region all along the chord. Similar findings are reported in Ref. 1 for the global thermo-mechanical stress analysis of selected time slices after entry interface for a given mission trajectory. Additional simulations are also reported in Ref. 1 that included a piecewise linear through-the-thickness temperature variation. Those simulations indicate the predicted small non-uniform through-the-thickness variation gives only a small increase in the predicted thermo-mechanical stresses compared to those predicted using a uniform through-the thickness temperature distribution.

Figure 11. Substrate through-the-thickness normal stress distributions along the lower-apex region of slip-side joggle region at the coating-substrate interface for the best-estimate stress-free temperature for three thermal loading conditions.
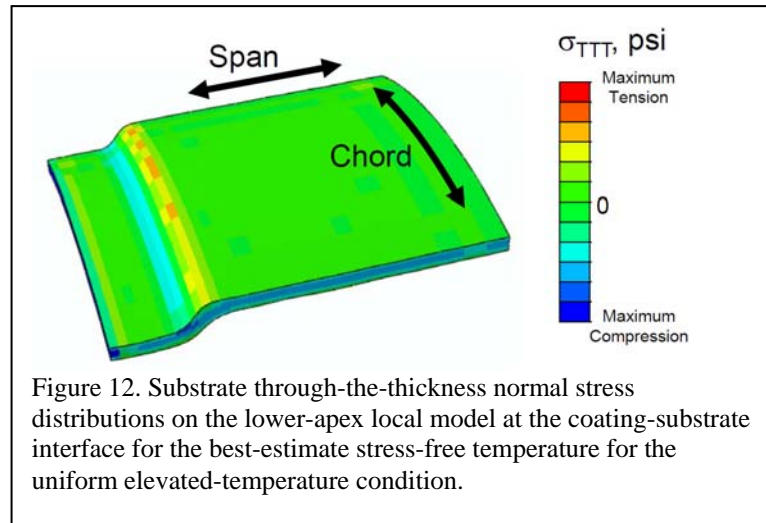
C. Lower-Apex Local Model

Next, a local joggle segment just below the panel apex and along the slip-side joggle extracted from the global three-dimensional stress analysis model is examined. Since the slip-side joggle region is of primary interest, the entire panel rib region of the local segment shown in Figure 3 is excluded from the local isolated model. Using such an isolated three-dimensional joggle segment, the influence of several modeling and analysis factors can be examined, see Ref. 8. The results are then compared to those obtained from the global Panel 10 model for the same slip-side joggle region and for the same uniform thermal condition, i.e., Fig. 11c. Note that on the local model, the boundary conditions that remove the rigid body motion are prescribed.

The isolated local lower-apex model tends to predict nearly the same peak tensile substrate σ_{TTT} stress levels compared to those obtained using the global panel model – compare Figs. 11c and 12, except for edge effects in the

local model. Second, the substrate through-the-thickness response predicted for the local model is nearly uniform in the chord direction. This finding indicates that the use of simple boundary conditions (i.e., just remove the rigid-body motion) is sufficient to generate a substrate through-the-thickness response similar to the global response for uniform thermal conditions.

Figure 12. Substrate through-the-thickness normal stress distributions on the lower-apex local model at the coating-substrate interface for the best-estimate stress-free temperature for the uniform elevated-temperature condition.

IV.   Concluding Remarks

The thermo-mechanical elastic stress analyses of a wing-leading-edge (WLE) reinforced carbon-carbon (RCC) panel assembly are presented for selected end-of-mission entry thermal conditions. Modeling and analysis details related to material modeling, attachment hardware modeling, geometric configurations, and thermal loading are summarized. Numerical results are presented for three thermal conditions.

Results from these simulations indicate that along the coating-substrate material interface, the substrate through-the-thickness normal stress and strain values have a higher value than is found within the substrate. These values tend to increase as the slip-side joggle region is approached from the panel acreage region. The magnitude of these values is dependent on the local applied temperature and the assumed value for the stress-free temperature of the material. The substrate through-the-thickness stress and strain values increase as the stress-free temperature decreases. This change in response is approximately proportional to the change in local applied temperature relative to the stress-free temperature.

For the integrated global analyses, the interaction between the panel edges and the intermediate T-seal is found to be minimal for the thermal conditions analyzed. Hence, isolated WLE panels can be analyzed to determine the entry thermo-mechanical stress response. No localized 'hot spots' were identified on the panel for the entry heating cases. However, increased stress levels were observed *all along* the slip-side joggle shoulder region. The global three-dimensional stress analysis also showed that this increase in stress in the joggle shoulder was independent of chord location and dependent on the local temperature. Results from the global analysis using a specified uniform temperature confirmed that the increase in stress in the slip-side joggle region was not dependent on location along the panel chord direction.

Results from the global three-dimensional panel models were compared with independent local three-dimensional model results. The through-the-thickness stress and strains were determined to be comparable for the two models using simple boundary conditions for the local three-dimensional model. These local three-dimensional models also show that the stresses do not exhibit any variation in the chord direction except near the local model boundaries. Thus, a two-dimensional spanwise slice through the RCC thickness near the slip-side joggle at the panel apex can be taken out of the panel, and that slice can be modeled using two-dimensional plane-strain assumptions. Plane-strain models are anticipated to be used to determine the spanwise and through-the-thickness variations of the thermo-

mechanical response to uniform thermal loading conditions as well as to assess the effect of subsurface defects from a fracture mechanics perspective.

References

1. Knight, N.F., Jr., Song, K., and Raju, I. S., *Global Thermo-Mechanical Stress Analysis of Space Shuttle Orbiter Wing-Leading-Edge Panels*, NASA TM/2010-215925, 2010.

2. Knight, N. F., Jr., Song, K., Moore, D. F., and Raju, I. S., *Space Shuttle Orbiter Wing-Leading-Edge Panel Assembly Description and Attachment Hardware Modeling*, NASA TM/2010-215918, 2010.

3. Anon., *ABAQUS Analysis User's Manual: Volumes I – VI*, Version 6.7, Dassault Systèmes Simulia Corp., Providence, RI, 2007.

4. Raju, I. S., Song, K., Knight, N. F., Jr., and Phillips, D. R., *Fracture Mechanics Analyses of the Slip-Side Joggle Region of the Space Shuttle Orbiter Wing-Leading-Edge RCC Panels*, NASA/TM-2010-215922, 2010.

5. Raju, I. S., Phillips, D. R., Knight, N. F., Jr., and Song, K., "Fracture Mechanics Analyses Reinforced Carbon-Carbon Wing-Leading-Edge Panels," AIAA Paper No. 2010-2689, April 2010.

6. Raju, I. S., Phillips, D. R., and Knight, N. F., Jr., *Stress-Free Temperature Prediction for Reinforced Carbon-Carbon*, NASA TM/2010-215919, 2010.

7. Knight, N. F., Jr., *User-Defined Material Model for Thermo-Mechanical Progressive Failure Analysis*, NASA CR-2008-215528, November 2008.

8. Knight, N.F., Jr., Song, K., and Raju, I. S., *Factors Influencing Thermo-Mechanical Elastic Response of Slip-Side Joggle Regions of the Space Shuttle Orbiter Wing-Leading-Edge Panels*, NASA TM/2010-215926, 2010